

# CFD EVALUATION AGAINST A LARGE SCALE UNCONFINED HYDROGEN DEFLAGRATION

Tolias, I.C.<sup>1,2</sup>, Venetsanos, A.G.<sup>1</sup>, Markatos, N.<sup>2</sup> and Kiranoudis, C.T.<sup>2</sup>

<sup>1</sup> Environmental Research Laboratory, National Center for Scientific Research Demokritos, Agia Paraskevi, 15310, Greece, [tolias@ipta.demokritos.gr](mailto:tolias@ipta.demokritos.gr), [venets@ipta.demokritos.gr](mailto:venets@ipta.demokritos.gr)

<sup>2</sup> National Technical University of Athens, School of Chemical Engineering, Heroon Polytechniou 9, Zografou, 15780, Greece, [n.markatos@ntua.gr](mailto:n.markatos@ntua.gr), [kyr@chemeng.ntua.gr](mailto:kyr@chemeng.ntua.gr)

## ABSTRACT

In the present work, CFD simulations of a large scale open deflagration experiment are performed. Stoichiometric hydrogen-air mixture occupies a 20 m hemisphere. Two main combustion models are compared and are evaluated against the experiment. The Eddy Dissipation Model and a multi-physics combustion model which is based on Yakhot's equation for the turbulent flame speed. The values of models' critical parameters are investigated. The effect of the turbulence model on the results is also examined. LES approach and k- $\epsilon$  model were tested. The multi-physics combustion model using the RNG LES turbulence model achieved the best agreement with the experiment.

## 1.0 INTRODUCTION

During the last several years hydrogen has been a subject of massive research as a potential energy carrier. If hydrogen is to be used in practical applications, a thorough risk assessment is required since it is a flammable gas capable of causing deflagrations or even detonations. For this purpose Computational Fluid Dynamics (CFD) may be an accurate and reliable numerical tool for performing safety assessment. Any CFD code should be validated, before practical use, in order to evaluate its capabilities and limitations.

In this work, two types of combustion models, the Eddy Dissipation Model and a multi-physics combustion model, and two kinds of turbulence models, LES approach and k- $\epsilon$  model, are evaluated against a large scale open deflagration experiment. A hydrogen-air mixture of 29.7% by volume occupies an unconfined hemispherical volume of 20 m diameter. The experiment was conducted by the Fraunhofer Institute for Propellants and Explosives and it was the largest unconfined hydrogen-air deflagration ever performed [1]. The simplicity and the scale of this experiment makes it a very good benchmark exercise in order to evaluate models for hydrogen safety studies. Explosion pressure was measured at 2.0, 3.5, 5.0, 6.5, 8.0, 18.0, 25.0, 35.0, 60.0 and 80.0 m from the ignition point which it was located at the center of the hemisphere. More details about the experiment may be found in [1].

The same experiment was simulated earlier by Molkov et al. (2006) [1], Molkov et al. (2007) [2] and Garcia et al. (2010) [3], by using various models and computer codes. The present paper presents for the first time, to the authors' best knowledge, a comparison of different combustion and turbulence models with the above experiment, by using the same CFD code. As a result, a consistent comparison among the models can be made by excluding the effects of different grids, numerical schemes etc. This work was done in the framework of the SUSANA project [4]. The modeling strategy is based on the guide to best practices in numerical simulations [5] that is being developed within the SUSANA project.

## 2.0 MATHEMATICAL METHODOLOGY

### 2.1 Governing equations

The model used solves the space-averaged Navier-Stokes equations along with the energy equation (conservation equation of static enthalpy) and the conservation equation of each of the mass fraction of the species that take part in the combustion process. The multi-component mixture is assumed to be in thermodynamic equilibrium. The equation of state for ideal gases relates pressure with density and

temperature. The set of the main equations that was used are presented in [6], while for the CFD simulations the ADREA\_HF code was used [7].

The main issue in deflagration modeling is the estimation of the reaction rate which appears in the equation of species as source term. The combustion process occurs typically in a very thin area (flame front) which propagates in space over time. In real case scenarios, this area is very small compared to the length scale of the problem. Consequently, direct numerical simulation with detailed chemistry is not possible at present. As a result, models for the estimation of the reaction rate need to be used. Two main combustion models are compared in the present work: The ‘‘Multi-phenomena turbulent burning velocity’’ model, and the ‘‘Eddy Dissipation Concept (EDC)’’ model.

The ‘‘Multi-phenomena turbulent burning velocity’’ model [8] is based on the turbulent flame speed concept. The turbulent flame speed is calculated based on a modification of Yakhot's equation, in order to account for all the main physical mechanisms which appear in hydrogen deflagrations such as the turbulence generated by the flame front itself, preferential diffusion and fractal structure of the flame front:

$$S_t = \Xi_k \cdot \Xi_{lp} \cdot \Xi_f \cdot S_u \cdot \exp\left(\frac{u'}{S_t}\right)^2 \quad (1)$$

where  $S_t$  is the turbulent flame speed,  $S_u$  the laminar flame speed (as a function of pressure)  $u'$  the sub-grid scale or the fluctuating velocity component and  $\Xi$  are factors that account for the various mechanisms which accelerate the combustion process. Details about the implementation in the ADREA\_HF can be found in [6]. The values of the main parameters that were used in the present simulations are:

$$\Xi_k^{\max} = 3.6, \quad R_0 = 1.2 \text{ m}, \quad \psi = 0.5, \quad S_{u0} = 1.96 \text{ m/s}, \quad \varepsilon = 0.565, \quad \Xi_{lp} = 1.25 \quad (2)$$

where  $\Xi_k^{\max}$  is the maximum value of the wrinkling factor,  $R_0$  the critical radius where the turbulence is fully developed,  $\psi$  a model constant,  $S_{u0}$  the laminar flame speed at initial conditions,  $\varepsilon$  the overall thermo-kinetic index and  $\Xi_{lp}$  the factor which accounts for the leading point concept [9]. The  $\Xi_f$  coefficient which accounts for the enhancement of the flame surface due to its fractal structure, is given by the equation:

$$\Xi_f = \begin{cases} \left(\frac{R}{R_0}\right)^{D_f-2}, & R \geq R_0 \\ 1, & R < R_0 \end{cases} \quad (3)$$

where  $R$  is the distance from the ignition point and  $D_f$  the fractal dimension. Various values of the fractal dimensions have been proposed in the literature. The majority of the suggested values lies between 2.05 and 2.35. North and Santavicca [10] related fractal dimension with flow turbulence and they proposed the following equation:

$$D_f = \frac{2.05}{u'/S_u + 1} + \frac{2.35}{S_u/u' + 1} \quad (4)$$

For low values of  $u'/S_u$  (low turbulence) fractal dimension tends to 2.05, whereas for high values of  $u'/S_u$  (high turbulence) fractal dimension tends to 2.35.

A simpler variation of the above model, here called ‘‘Simplified turbulent burning velocity’’ model, which does not include the fractal sub-model is also used, in order to exploit the significance of the fractal sub-model in the current application. The leading point concept is not included too. The turbulent burning velocity is estimated by the equation:

$$S_t = \Xi_k \cdot S_u \cdot \exp\left(\frac{u'}{S_t}\right)^2 \quad (5)$$

This model was used also in [1]. In [1], a value of  $\psi$  equal to 1.0 is suggested and this value is also used here. The different values of the constant between the former and the latter model can be explained by the fact that these are two different models. In the latter model, the  $\Xi_k$  coefficient can be considered as a ‘‘global’’ wrinkling factor which includes the effects of the leading point concept and the fractal structure of the flame front. These effects are modelled with separately factors ( $\Xi_{ip}$  and  $\Xi_f$ ) in the former model. As a result, a higher value of the constant is required in the ‘‘Simplified turbulent burning velocity’’ model compared to the ‘‘Multi-phenomena turbulent burning velocity’’ model.

The second combustion model which is evaluated is the ‘‘Eddy Dissipation Concept (EDC)’’ [11]. EDC is a widely used model due to the fact that the reaction rate is written as a simple function of known mean quantities without the need of solving additional transport equations. The main assumption of this model is that turbulence drives the combustion process. The reaction rate is a function of the inverse of the integral turbulence time scale:

$$\bar{\omega} = C_{EDC} \rho \frac{\varepsilon}{k} \min \left[ \frac{Y_f}{\nu_f MW_f}, \frac{Y_{O_2}}{\nu_{O_2} MW_{O_2}}, \frac{\sum_{i=1}^{np} Y_i}{\sum_{i=1}^{np} \nu_i MW_i} \right] \quad (6)$$

where  $C_{EDC}$  is the model constant,  $\rho$  the mixture density,  $\varepsilon$  the turbulence dissipation rate,  $k$  the turbulence kinetic energy,  $Y$  is the mass fraction,  $\nu$  the stoichiometric coefficient,  $MW$  the molecular weight and  $np$  the number of products. The subscripts  $f$  and  $O_2$  account for the fuel and oxygen. Flame extinction has not been included in the model, as it has not been expected to occur in hydrogen premixed flames, especially in unconfined geometries.

The RNG LES turbulence model was used along with the ‘‘Multi-phenomena turbulent burning velocity’’ model and the ‘‘Simplified turbulent burning velocity’’ model, whereas the k- $\varepsilon$  turbulence model was used along with the EDC model. The k- $\varepsilon$  turbulence model is chosen to be used along with the EDC model for two reasons: 1) The original EDC model [11] is strongly dependent on  $k$  and  $\varepsilon$  values and as a result k- $\varepsilon$  model seems to be more appropriate and 2) k- $\varepsilon$  model has been widely used along with the EDC model.

Finally, the effect of the turbulence model was examined for the ‘‘Multi-phenomena turbulent burning velocity’’ combustion model. The RNG LES model, the standard k- $\varepsilon$  model and the RNG k- $\varepsilon$  model were studied.

## 2.2 Grid and domain-size

Various domain-sizes were studied in order to examine the impact on the results. The domain-sizes that were tested are presented in Table 1. Furthermore, three different grids were used to perform the grid independence study. ADREA-HF uses Cartesian grids. The number and the size of cells are presented in Table 2. The cells’ volume is increased gradually in the area away from the hydrogen-air

mixture (expansion ratio from 1.08 to 1.12) in order to save computational time. Grid cells at the area of the bottom of the hemisphere ( $z=0$  plane) are shown in Fig. 1.

Table 1. Dimensions of the numerical domain

|          | Length (m) | Width (m) | Height (m) |
|----------|------------|-----------|------------|
| Domain 1 | 200        | 200       | 100        |
| Domain 2 | 300        | 300       | 150        |
| Domain 3 | 400        | 400       | 200        |

Table 2. Grid characteristics

|                      | Number of cells (Domain 1) | Cell size                               |
|----------------------|----------------------------|---|
| Grid 1 (coarse grid) | 442,225                    | 1.0 m cell size inside hemisphere       |
| Grid 2 (fine grid)   | 953,127                    | 0.5 m cell size inside hemisphere       |
| Grid 3 (finer grid)  | 1,371,791                  | 0.25 to 0.5 cell size inside hemisphere |

### 2.3 Numerical details

ADREA-HF uses the finite volume method on a staggered Cartesian grid. A difficulty in this kind of mesh is how to define accurately the initial conditions in the hemisphere. In order to define the hemisphere area in which the initial hydrogen-air mixture exists, the following strategy was followed: In cells which are totally inside the hemisphere the mass fractions are calculated based on the 29.7% v/v hydrogen-air concentration. In cells which are partially inside the hemisphere we first estimate (numerically) the volume of the blocked part of the cell (i.e. the volume of the union of cell with sphere) and then we “distribute” the mass of the blocked part of the cell in the whole cell and we calculate the new mass fractions. In Fig. 1 the initial hydrogen mass fraction contours are shown. We observe that an almost circular shape of the initial distribution is achieved even with the coarse grid.

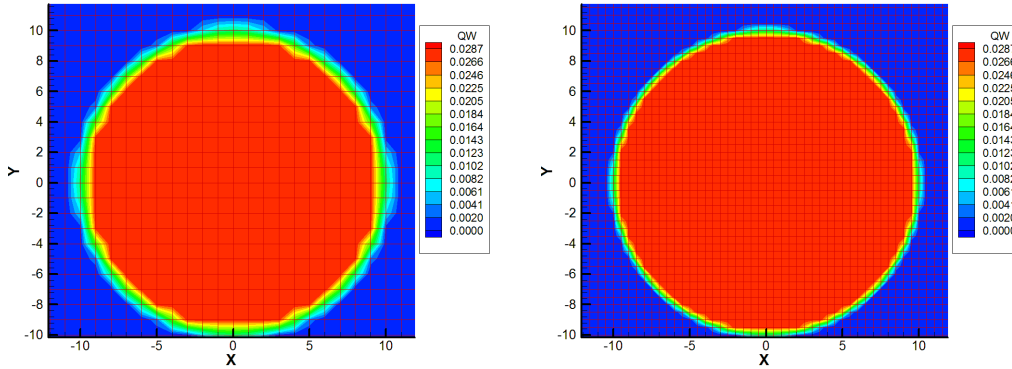


Figure 1. Hydrogen mass fraction contours at  $z=0$  plane for the coarse (left) and the fine (right) mesh at initial conditions.

The pressure and velocity equations are decoupled using a modification of the SIMPLER algorithm. For the discretization of the convective terms in the momentum equations a second order accurate bounded central scheme was used while in the conservation equations of species and energy a second order accurate bounded linear upwind scheme. The implementation was carried out using a deferred-correction approach via the source term. For the time advancement, the second order accurate Crank-Nicolson numerical scheme was chosen. The time step is automatically adapted according to prescribed error bands and the desired Courant–Friedrichs–Lewy (CFL) number. CFL maximum value was set equal to 0.8.

At all exit planes (lateral, front, back and top) the non-reflecting type boundary conditions for the normal velocities is chosen, while for the parallel to the exit planes' velocity components, zero gradient boundary conditions are applied. Zero gradient is utilized also for the mass fraction of species. As initial conditions, a stagnant flow field with no turbulence is specified. Initial temperature and pressure were set equal to experimental values, i.e. 283 K and 98900 Pa respectively. In the hydrogen-air premixed area an initial mass fraction of hydrogen and oxygen is specified, as described above. Outside this area the mass fraction of oxygen is set equal to 0.2329. Nitrogen is the inert specie. Ignition is modelled by fixing the reaction rate in a cell at the ignition point, in order the initial amount of fuel to be burned at a determined interval. This interval is estimated by the formula  $\frac{Dx/2}{E \cdot S_{u0}}$  where

$Dx$  the size of the cell at ignition point,  $E = 7.2$  the expansion coefficient and  $S_{u0} = 1.96 \text{ m/s}$  the laminar burning velocity at the initial pressure. The ignition was modelled with exactly the same way in all simulations.

For the simulations a modern processor (Intel i7-2600K, 3.4GHz) with 4 real cores was used. The simulations run parallel in all 4 cores. The computational time was approximately equal to 14 hours when the Grid 1 was used and 27 hours when Grid 2 was used.

### 3.0 RESULTS AND DISCUSSION

#### 3.1 Grid-independency and domain-size sensitivity study

The grid-independency and the domain-size sensitivity study was made by using the ‘‘Simplified turbulent burning velocity’’ model. In Fig. 2 the pressure at 5 and 80 meters from the center of the hemisphere is presented for the three different grids. The Domain 1 was used. We observe that the results are almost identical among grids. The same behavior is observed for the rest of the sensors (at 2, 8, 18 and 35 m). Thus, grid-independency is achieved even with the coarse grid.

In Fig. 3 the pressure at 5 and 80 meters from the center of the hemisphere is presented for the three different domain sizes. The Grid 1 was used. We observe that the domain size has a significant impact on the results at the closest to the boundary sensor (80 m). At the sensor positioned at 5 meters, the extended domains affect the results only at the tail of the pressure-time curve. This behavior is also observed at the rest of the sensors (at 2, 8, 18 and 35 m). When the Domain 1 is used (200 x 200 x 100 m), the pressure fails to return to its initial value. Domains 2 and 3 (extended domains), however, reproduce this physical behavior. Small differences between Domain 2 and 3 are observed only at the tail of the pressure-time curve at the last position (80 m). At that sensor, even the Domain 2 fails to restore the initial value of the pressure and the more extended Domain 3 is required. However, this difference is not all that significant and thus the Domain 2 will be used for the rest of analysis.

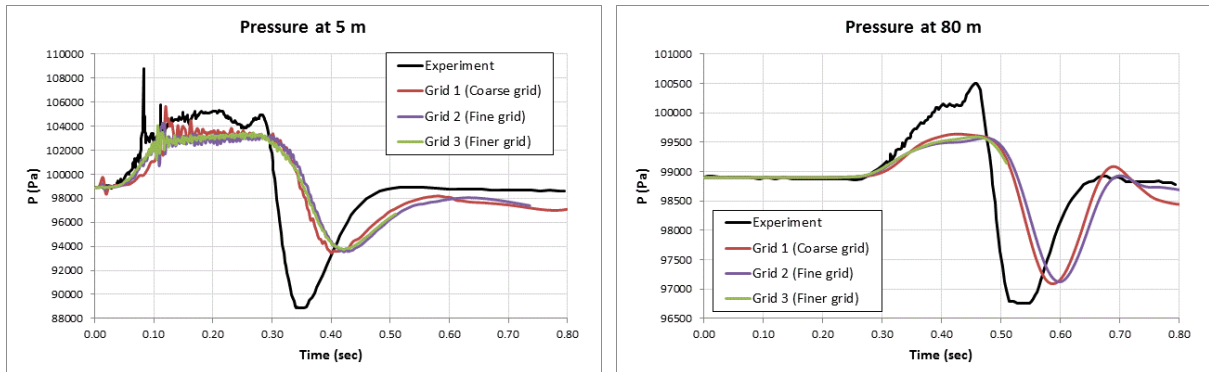


Figure 2. Pressure at 5 and 80 m from the center of the hemisphere, for three different grids (on Domain 1) - ‘‘Simplified turbulent burning velocity’’ model.

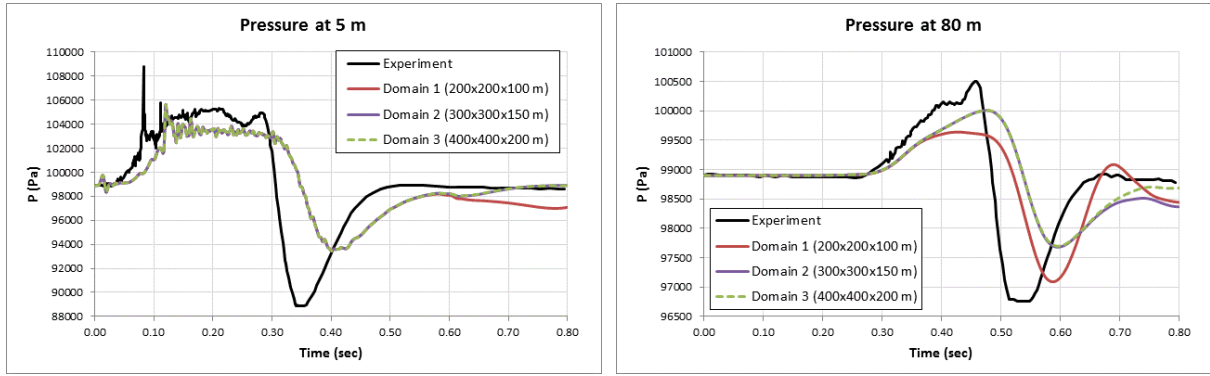
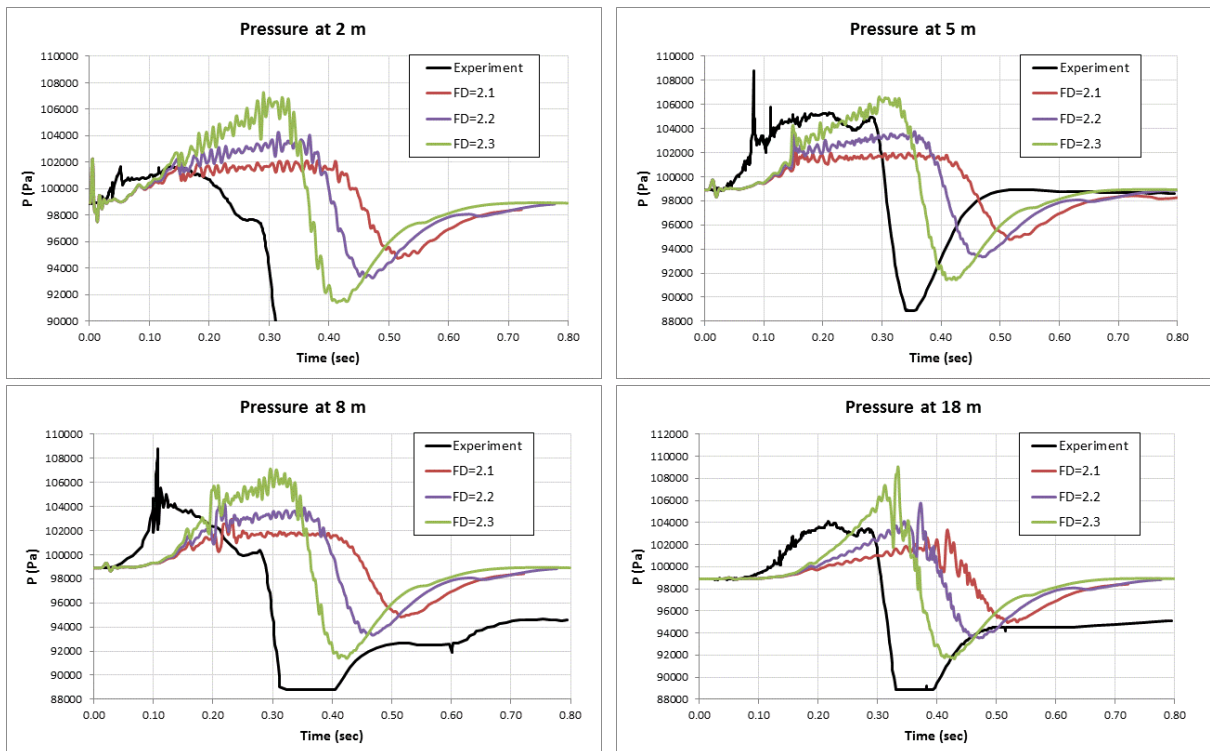


Figure 3. Pressure at 5 and 80 m from the center of the hemisphere, for three different domain sizes (on Grid 1).

### 3.2 Fractal dimension sensitivity study

The coarse mesh and the extended domain (Domain 2) were used for the “Multi-phenomena turbulent burning velocity” model simulations. A key parameter of this model is the fractal dimension. In Fig. 4 the pressure time histories for three different values of the fractal dimension (2.1, 2.2 and 2.3) are compared against the experiment. We observe that the results are strongly depend on the fractal dimension value. The best agreement with the experiment is obtained with the value of 2.3 for most of the sensors.

The semi-empirical relation for fractal dimension (equation 4) is also tested. In Fig. 5 the model using this relation is compared (for the sensors at 5 and 80 m) with the model using constant values of the fractal dimension. We observe that the results of the semi-empirical relation lie between the results of constant fractal dimension equal to 2.1 and 2.2. Consequentially, the empirical relation fails to approximate the value of 2.3 for which the best agreement with the experiment was achieved.



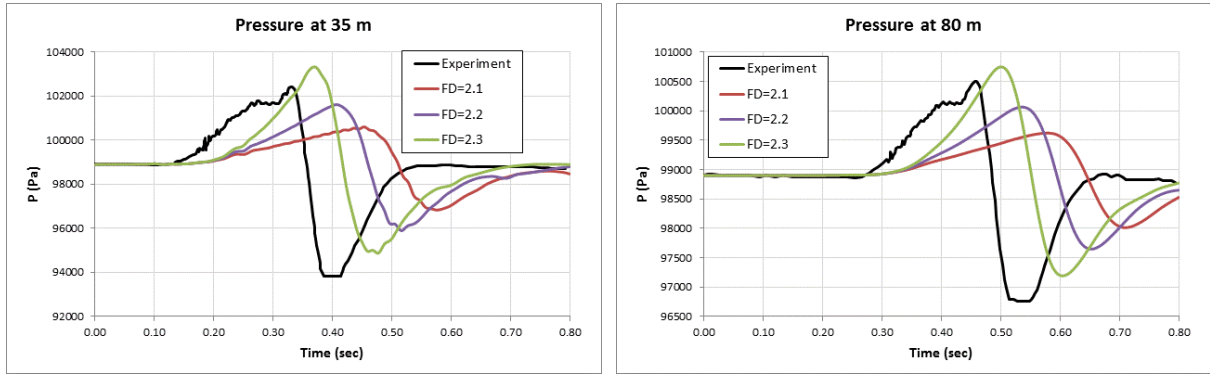


Figure 4. Pressure at 2, 5, 8, 18, 35 and 80 m from the center of the hemisphere, for three values of fractal dimension - “Multi-phenomena turbulent burning velocity” model.

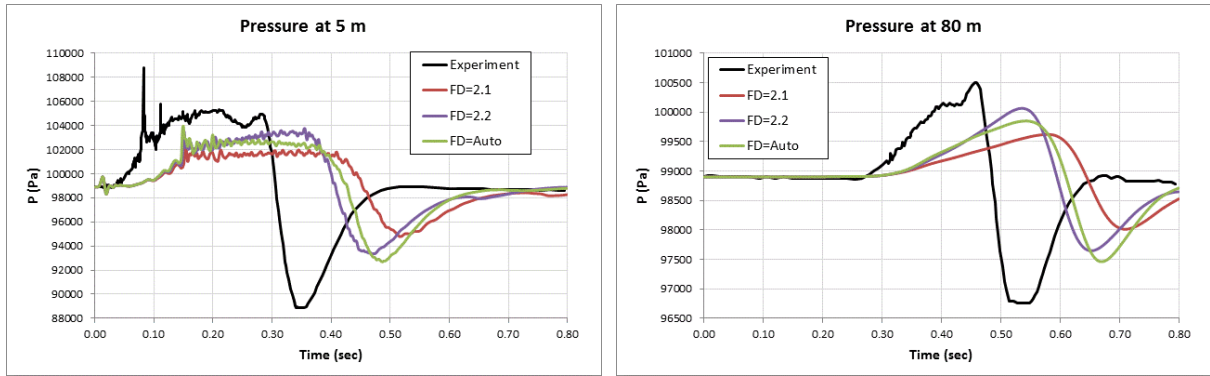


Figure 5. Pressure at 5 and 80 m from the center of the hemisphere - Comparison of the Fractal semi-empirical relation with the constant values model.

### 3.3 Combustion models comparison

In Fig. 6 the comparison among the three combustion models is shown. Two main parameters against which two deflagration models should be compared in order to evaluate them are: the maximum/minimum pressure and the rate of pressure rise/fall. A secondary parameter is the time at which the maximum pressure occurs. We focus the model comparison only on results at the 5, 35 and 38 m sensors. At the other positions we observe that the experimental pressures fail to return to their initial values and that the pressure curve at the area of the negative pressure peak has an unexpected form. Consequently, the experimental measurements at these positions are not considered reliable to compare with.

The value of the constant for the EDC model for which the best results were achieved was 1.8. A sensitivity study for the value of this constant revealed a strong dependency of the results on this value. This is a significant drawback of the model. Another drawback of the model is the dependency on the initial values of  $k$  and  $\varepsilon$ . Small initial values for both variables equal to  $10^{-6}$  were chosen in the current simulation.

Regarding the maximum pressure (neglecting the oscillations), we observe that at 5 m a small overprediction for the multi-phenomena model (with fractal dimension equal to 2.3) occurs whereas “Simplified turbulent burning velocity” and EDC combustion models under-predict the experimental value. The same behavior is observed at the sensors at 35 and 80 m. At these two positions EDC model under-predicts the pressure more than the simplified model. Concerning the minimum pressure value, all models over-predict the experimental value. However, the multi-phenomena model is closer to the experiment. “Simplified turbulent burning velocity” model produces the next best solution. Regarding the rate at which the pressure falls, the multi-phenomena model achieves the best

agreement with the experiment at all sensors. Simplified model predicts smaller rates and EDC even smaller. Regarding the rate at which the pressure rise, at 35 and 80 m the multi-phenomena and the EDC model have similar behavior, whereas the simplified model predicts smaller rates. Finally, concerning the time arrival of the pressure peak, a small delay on the multi-phenomena model is observed. The “Simplified turbulent burning velocity” model achieves the best agreement with the experiment at all sensors.

Overall, the “Multi-phenomena turbulent burning velocity” model with fractal dimension equal to 2.3 achieves better agreement with the experiment, both in terms of maximum/minimum pressure and in terms of rate of pressure rise/fall which are the most significant parameters in deflagration modeling.

In Fig. 7 the flame radius as a function of time is depicted for the three combustion models. Comparing the multi-phenomena model with the simplified model, we observe that the first one predicts the acceleration of the flame front, whereas the simplified model fails. The fractal sub-model of the multi-phenomena model is responsible for this acceleration. EDC model also predicts the acceleration of the flame front, however, a time delay is observed. The above behavior is in agreement with the rate of the pressure rise, where the simplified model under-predicts it while the other two models predict it more accurately.

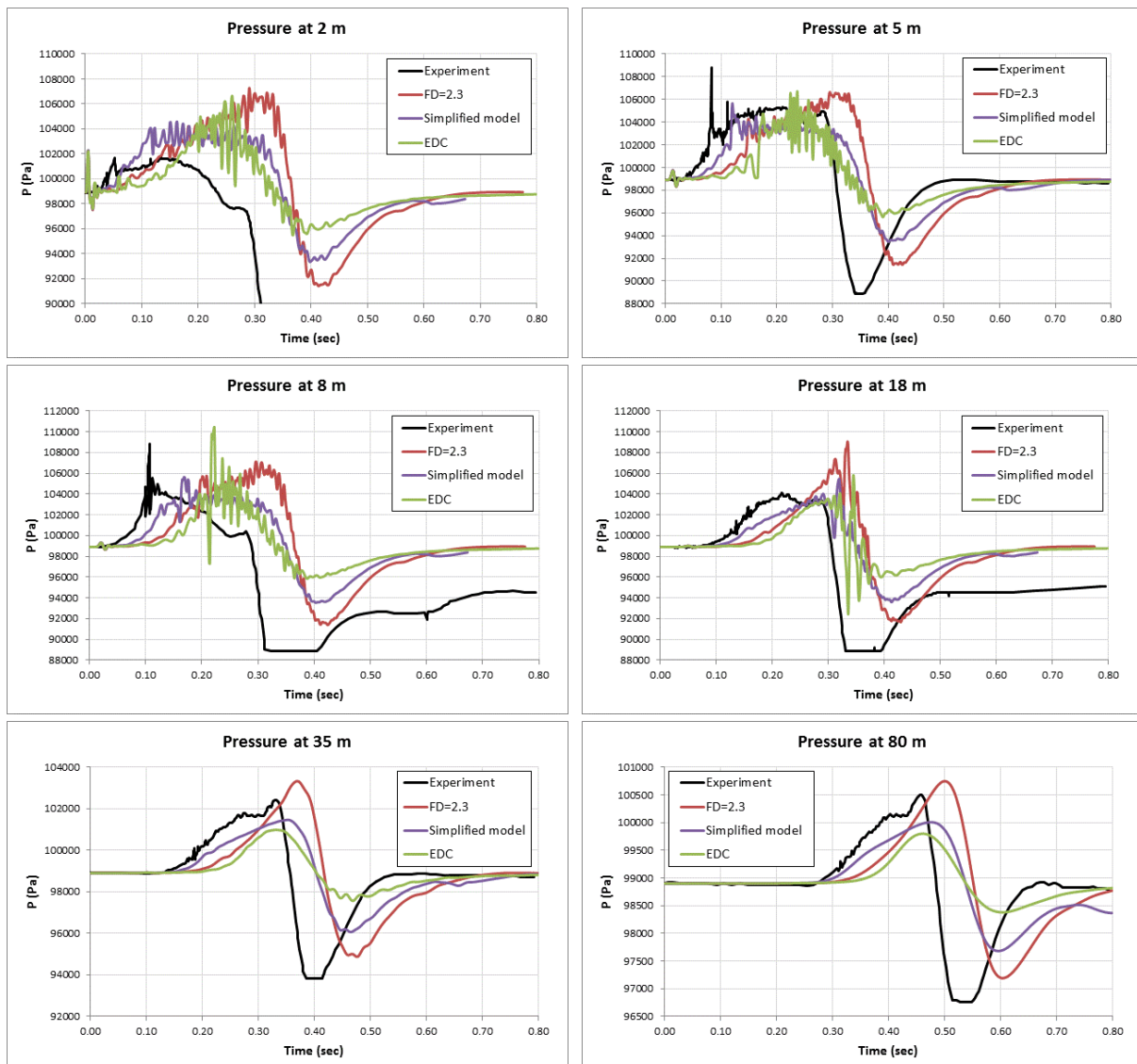




Figure 6. Pressure at 2, 5, 8, 18, 35 and 80 m from the center of the hemisphere - Combustion model comparison.

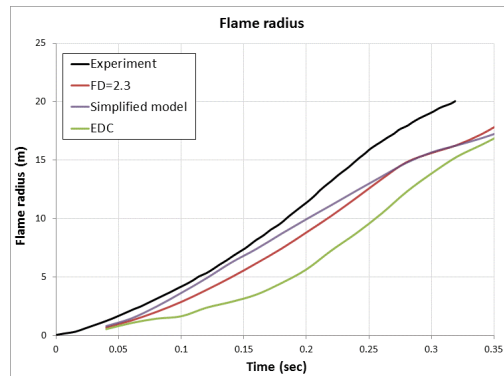
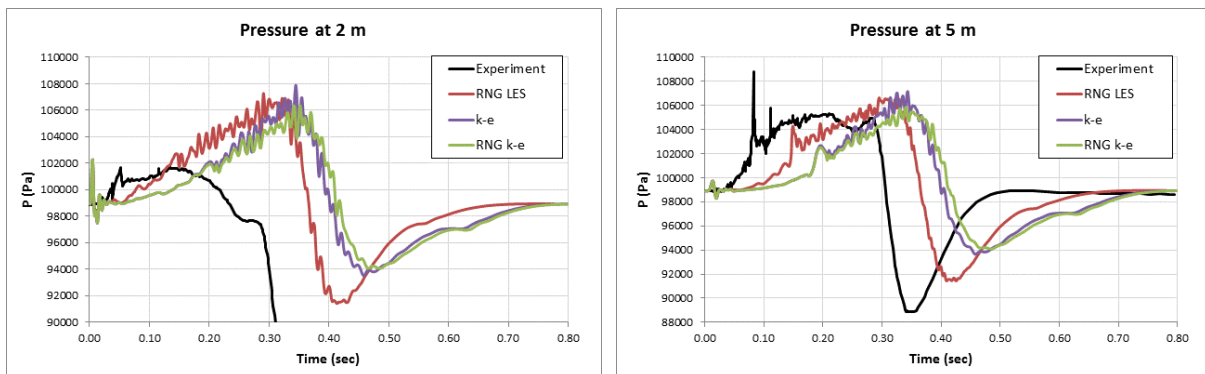


Figure 7. Flame radius as a function of time for the three combustion models.

### 3.4 Turbulence models comparison

The effect of the turbulence model was examined along with the “Multi-phenomena turbulent burning velocity” combustion model; the RNG LES model, the standard k- $\epsilon$  model and the RNG k- $\epsilon$  model were used for this comparison. In Fig. 8 the comparison between the turbulence models is shown. Two main differences are observed between the LES model and the k- $\epsilon$  models: 1) A time delay is noticed in the case of both the k- $\epsilon$  models and 2) the minimum pressure peak is over-predicted by the k- $\epsilon$  models. The main reason for the time delay is the predicted values of  $u'$ . As shown in Fig. 9, the RNG k- $\epsilon$  model predicts lower values of  $u'$  compared to the RNG LES model. The maximum value of  $u'$  that the RNG LES predicts can not be achieved with the k- $\epsilon$  model even at later times. The RNG LES model calculates large values of  $u'$  at the ‘ring’ where the combustion takes place, whereas the RNG k- $\epsilon$  model predicts large values of  $u'$  only near the ground. The main parameter of the combustion model which drives turbulent flame speed at the initial stage of combustion is  $u'$ . As a result, small values of  $u'$  at the initial stages lead to a delayed maximum overpressure. The lower values of  $u'$  have also a small impact on the maximum overpressure and on the rate of pressure rise. The same behavior has been observed in [6]. Finally, comparison of the standard k- $\epsilon$  model with the RNG k- $\epsilon$  model reveals only minor differences.



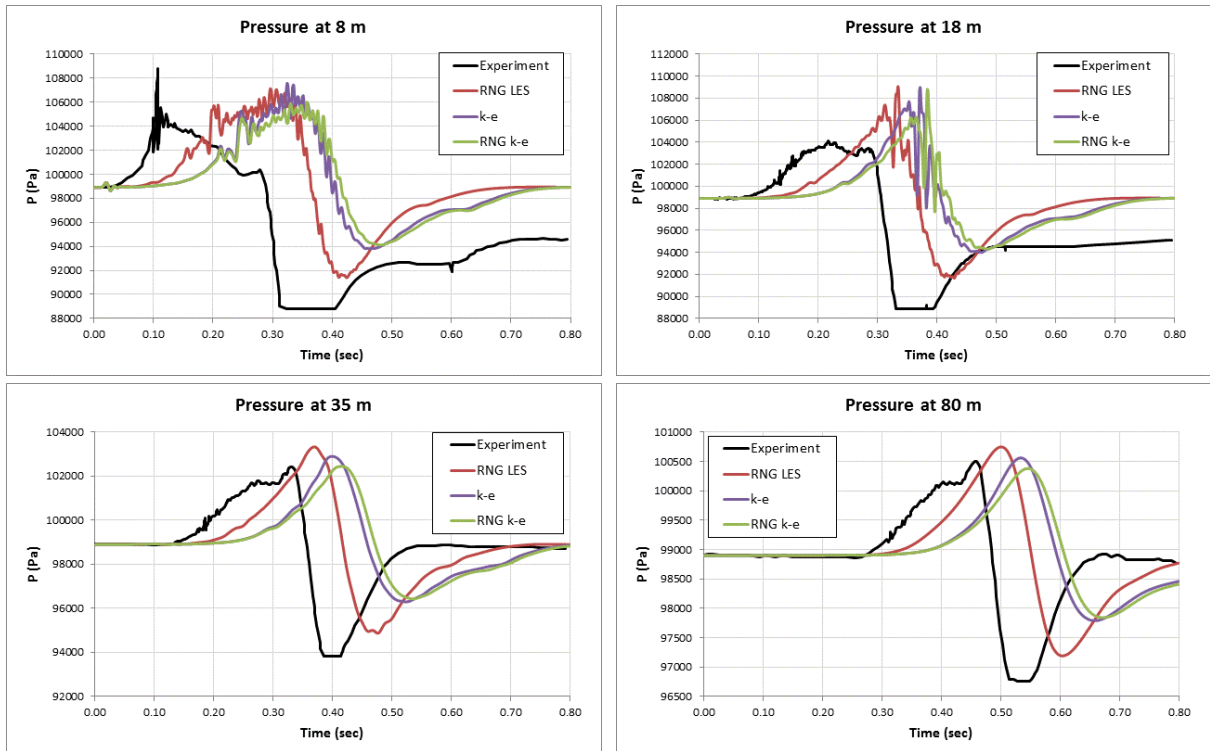


Figure 8. Pressure at 2, 5, 8, 18, 35 and 80 m from the center of the hemisphere - Turbulence model comparison.

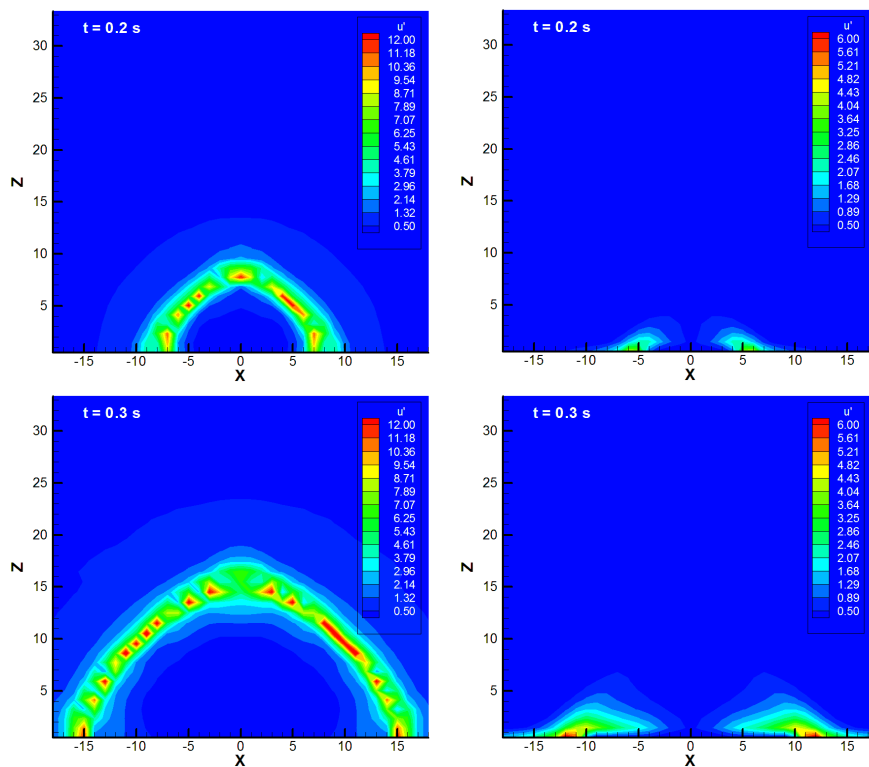


Figure 9. Subgrid scale or fluctuating velocity contours at the plane  $y=0$  (center of the hemisphere) at  $t=0.2$  s and  $t=0.3$  s for the RNG LES (left) and the RNG  $k-\epsilon$  (right) case.

## 4.0 CONCLUSIONS

A large scale open deflagration experiment was simulated using two main combustion models: the “Multi-phenomena turbulent burning velocity” model and the EDC model. A simpler variation of the multi-phenomena model, was also tested. The effect of grid and domain size was examined. The grid with 1.0 m cell size inside the hemisphere was found to be appropriate for simulating the generated overpressures. A domain size of 300 x 300 x 150 m needs to be used in order to achieve results unaffected from the boundaries. A parametric analysis for the fractal dimension parameter of the multi-phenomena model was performed. The value of 2.3 achieved the best agreement with the experiment. A semi-empirical relation for the fractal dimension was also tested. This relation failed to approximate the value of 2.3. The multi-phenomena model achieved very good agreement with the experimental results, better than both “Simplified turbulent burning velocity” model and EDC model. The multi-phenomena model and the EDC model both succeeded in reproducing the acceleration of the flame front. Finally, the effect of the turbulence model was examined for the multi-phenomena combustion model. The RNG LES model, the standard k- $\epsilon$  model and the RNG k- $\epsilon$  model were evaluated. The RNG LES model achieved the best agreement with the experiment. The k- $\epsilon$  models underestimated the values of the fluctuating velocity.

## ACKNOWLEDGEMENTS

The authors would like to thank the Fuel Cell and Hydrogen Joint Undertaking for the co-funding of the project SUSANA (“SUpport to SAfety ANalysis of Hydrogen and Fuel Cell Technologies”, Grant agreement no: 325386). The first author would also like to acknowledge the “IKY Fellowships of Excellence for Postgraduate Studies in Greece - Siemens Program” for the financial support.

## REFERENCES

1. Molkov, V., Makarov, D. and Schneider, H., LES modelling of an unconfined large-scale hydrogen–air deflagration, *J. Phys. D. Appl. Phys.*, **39**, No. 20, 2006, pp. 4366–4376.
2. Molkov, V., Makarov, D. and Schneider, H., Hydrogen-air deflagrations in open atmosphere: Large eddy simulation analysis of experimental data, *Int. J. Hydrogen Energy*, **32**, No. 13, 2007, pp. 2198–2205.
3. García, J., Baraldi, D., Gallego, E., Beccantini, A., Crespo, A., Hansen, O.R., Høiset, S., Kotchourko, A., Makarov, D. and Migoya, E., An intercomparison exercise on the capabilities of CFD models to reproduce a large-scale hydrogen deflagration in open atmosphere, *Int. J. Hydrogen Energy*, **35**, No. 9, 2010, pp. 4435–4444.
4. SUSANA project webpage, <http://www.support-cfd.eu/>.
5. Venetsanos, A.G., Talias, I.C., Giannissi, S.G., Coldrick, S., Ren, K., Kotchourko, A., Makarov, D., Chernyavsky, B. and Molkov, V, D3.1 Guide to best practices in numerical simulations, SUSANA project report, 2014.
6. Talias, I.C., Venetsanos, A.G., Markatos, N. and Kiranoudis, C.T., CFD modeling of hydrogen deflagration in a tunnel, *Int. J. Hydrogen Energy*, **39**, No. 35, 2014, pp. 20538–20546.
7. Venetsanos, A.G., Papanikolaou, E. and Bartzis, J.G., The ADREA-HF CFD code for consequence assessment of hydrogen applications, *Int. J. Hydrogen Energy*, **35**, No. 8, 2010, pp. 3908–3918.
8. Molkov, V.V., *Fundamentals of hydrogen safety engineering*, www.bookboon.com, 2012.
9. Zimont, V. and Lipatnikov, A., A numerical model of premixed turbulent combustion of gases, *Chem. Phys. Rep.*, **14**, No. 7, 1995, pp. 993–1025.
10. North, G.L. and Santavicca, D.A., The fractal nature of premixed turbulent flames, *Combust. Sci. Technol.*, **72**, No. 4–6, 1990, pp. 215–232.

11. Magnussen, B.F. and Hjertager, B.H., On mathematical modeling of turbulent combustion with special emphasis on soot formation and combustion, *Symp. Combust.*, **16**, No. 1, 1977, pp. 719–729.